J. Membrane Biol. 190, 43–56 (2002)
DOI: 10.1007/s00232-002-1022-8

The Journal of
Membrane
Biology

The Transport Systems of *Ventricaria ventricosa*: Hypotonic and Hypertonic Turgor Regulation

M.A. Bisson[1], **M.J. Beilby**[2]
[1]Department of Biological Sciences, State University of New York at Buffalo, Cooke Hall 109, Box 1300, Buffalo, NY 14260-1300, USA
[2]Biophysics Department, School of Physics, The University of NSW, Sydney 2052, Australia

Received: 17 November 2001/Revised: 29 May 2002

Abstract. The time course of hypertonic and hypotonic turgor regulation was studied in *Ventricaria* (*Valonia*) using pressure probe and *I/V*(current-voltage) analysis. Of 11 cells, 9 exhibited hypertonic turgor regulation, ranging from 100% regulation in 150 min to 14% regulation (14% recovery of the decrease in turgor) in 314 min. Some cells began regulating immediately, others took up to 90 min to begin. The resting *PD* (potential difference) became more positive in most cells. The *I/V* characteristics became more nonlinear with high resistance between −150 and −20 mV and negative conductance region near −70 mV. Prolonged (16 sec) voltage clamps to negative levels (−100 to −150 mV) showed progressively more rapid current turn-off, but subsequent *I/V* characteristics were not affected. Clamping to +150 mV, however, abolished the high conductance between −50 and +100 mV to yield a uniform high resistance *I/V* characteristic, similar to that in high $[K^+]_o$. Decreasing illumination from 2.02 μmol sec^{-1} m^{-2} to 0.5 μmol sec^{-1} m^{-2} had a similar effect. Two out of a total of three cells exhibited hypotonic turgor regulation. Both cells started regulating within minutes and achieved near 50% regulation within 50 min. The *PD* became more negative. The *I/V* curves exhibited high resistance between +50 and +150 mV. The characteristics were similar to those in cells exposed to low $[K^+]_o$. Prolonged voltage clamps to both negative and positive levels showed slow current increase. Decreased illumination increased the membrane resistance.

Key words: *Ventricaria* (*Valonia*) — Pressure probe — *I/V* analysis — Hypertonic and hypotonic turgor regulation — Electrogenic pump

Correspondence to: M.A. Bisson; email: bisson@acsu.buffalo.edu

Introduction

Previous experiments established that *Ventricaria* (formerly *Valonia*–Olsen & West, 1988) cells are capable of turgor regulation by assaying the vacuolar concentrations in cells acclimated to media of different osmolarities (Hastings & Gutknecht, 1976; Guggino & Gutknecht, 1982). In their elegant experiments, Hastings and Gutknecht (1974, 1976) showed that the active K^+ influx was induced by a decrease in turgor pressure rather than by a higher salt concentration. They suggested that the tonoplast contains a K^+ pump that is activated by low turgor pressure. Our investigation into the effect of changing $[K^+]_o$ on the *I/V* (current-voltage) characteristics revealed an unexpected response: low conductance in high $[K^+]_o$ and high conductance in low $[K^+]_o$ (Beilby & Bisson, 1999). Since K^+ channels should show an increase in conductance in high K^+, and are often activated by high K^+ medium (Beilby, 1986), this behavior supports the presence of the putative K^+ pump at the inner membrane. In this study, we investigate the unusual transporters of *Ventricaria* at the time of hypertonic and hypotonic stress. The pressure probe is an excellent tool for monitoring the cell turgor directly, as it can be applied for many hours with minimum effects on the cell and the regulation process. Thus the outcome, the change in the turgor pressure, can be correlated with the workings of the effector mechanisms, the ion pumps and channels, through *I/V* analysis.

The previous *I/V* analysis identified four major states, two of which are relevant to hypertonic and hypotonic regulation. The *I/V* profile that was associated with steady state in ASW and with hypertonic stress is nonlinear with a high-resistance region between −150 and −20 mV and high-conductance region centered near +50 mV. Upon exposure to the hypertonic medium, the resting *PD* becomes more

positive (from +6 mV to +18 mV in 6 cells in our previous study) and the nonlinear nature of the resting I/V profile is accentuated (Fig. 2 of Beilby & Bisson, 1999). A region of negative conductance is often observed between −100 and −50 mV, suggesting a strong *PD* dependence of the inactivation of the dominant transporter as the *PD* is clamped to more negative levels (Beilby, 1986). Previously we employed fast (100 msec pulse) I/V scans at the time of hypertonic regulation. In the present experiments, the investigations are extended to the time dependence of the clamp currents in the hypertonic state under prolonged voltage clamp.

The I/V profile associated with the hypotonic regulation displays the same features as the low $[K^+]_o$ profile: negative resting *PD* and high-resistance region between +50 and +150 mV. For cells in media with $[K^+]_o$ of 0.1 to 1.0 mM, we assumed that the cytoplasmic phase became depleted of K^+ due to the inward pumping of the putative K^+ pump at the tonoplast membrane. This assumption was supported by the observation that the typical low-$[K^+]_o$ I/V profile took about 20 min to develop. By this time, the K^+ pump could run out of substrate and not contribute to the I/V profile. We suggest that the negative-going *PD* opened K^+ channels on the tonoplast and that the plasmalemma K^+ channels are active in most states. Thus, this I/V profile is considered to represent "K^+ pump off, K^+ channels on." Such a configuration of transporters would be reasonable for a cell under hypotonic stress, where the vacuolar water potential needs to be increased by exporting K^+ and Cl^- from the vacuole. The hypotonic state is explored through fast I/V scans and prolonged voltage clamping.

Higher light intensity stimulates photosynthesis and production of ATP, in some cases also stimulating ion pumps (e.g., H^+ pump-mediated hyperpolarization in *Chara*, Fujii, Shimmen & Tazawa, 1979; Beilby, 1984; greater H^+ efflux from mesophyll tissues of bean leaves, Shabala & Newman, 1999; stimulation of an electrogenic H^+ pump in guard cells, Serrano, Zeiger & Hagivara, 1988, and tobacco mesophyll cells, Blom-Zanstra et al., 1997). The effect of light intensity is investigated in the present experiments to explore the behavior of the putative K^+ pump and possibly to distinguish it from channel-mediated effects.

Materials and Methods

The experiments described in this study were performed in Buffalo, NY, USA and Sydney, Australia. In the Buffalo experiments, the pressure probe was used to measure the vacuolar turgor pressure at the time of regulation. The vacuolar *PD* was also monitored. In the Sydney experiments, the current-voltage (I/V) characteristics were recorded at the time of regulation.

In the Buffalo experiments, cultures of *Ventricaria ventricosa* were generated from aplanospores from algae collected at Heron Island, Queensland, Australia. The aplanospores were removed from the mother cell with a sterile needle and cultured in conditioned artificial seawater that we received from the Aquarium of Niagara, Niagara Falls, New York. We filter-sterilized the seawater and enriched it with the supplement f/2 (Guillard & Ryther, 1962). The osmotic pressure of the medium was about 960 mOsmol kg^{-1}. Osmotic pressure was measured with a Wescor osmometer. Cells were grown under 50 μmol sec^{-1} m^{-2} white light, on a 14:10 light:dark cycle.

Cells for experiments were selected with diameters ranging from 2 to 4 mm. During the experiments, cells were bathed in a simplified artificial seawater, ASW, composed from (mM) 450 NaCl, 10 KCl, 50 $MgSO_4$, 8 $CaCl_2$, buffered to pH 8.0 with 10 HEPES (4-2[hydroxyethyl]-1-piperazine-ethane sulfonic acid) and NaOH, osmotic pressure of 990 mOsm kg^{-1}. The hypertonic stress was achieved by increasing the NaCl concentration to osmotic pressures up to 1200 mOsm kg^{-1}. Hypotonic stress was provided by decreasing the NaCl concentration to osmotic pressures down to 800 mOsm kg^{-1}. Cells were impaled with pressure probe only or simultaneously with a pressure probe and *PD*-measuring electrode as described in Stento et al. (2000). Briefly, the cell was impaled with a glass micropipette whose tip was beveled to give an opening of about 50 μm diameter, filled with silicone oil, and connected to a pressure transducer. The meniscus was controlled manually. Frequently the pipette tip clogged and the meniscus was difficult to move. In some cases, this resulted in a noisy trace due to overshoot and compensation when forcing the meniscus (*see* Fig. 1). Rarely, the overshoot would result in injection of silicone oil into the cell. In the short term, a small amount of oil did not harm the cell. If several droplets of oil were injected, in the long term they would coalesce and rise through the cell, coming to lodge just beneath the cell wall. If turgor began to fall, the experiment was terminated. In some experiments, cells were also impaled with a micropipette filled with 2 M KCl connected to a silver-silver chloride pellet to measure voltage. The impalement of the *PD*-measuring electrode caused the turgor to drop, with subsequent recovery. The cell was challenged by the osmotic change only after the turgor became steady.

In Sydney experiments, the diameter of cells ranged from 1 to 3 mm. *Ventricaria ventricosa* specimens were collected at Heron Island and transported to the laboratory at the University of New South Wales, where they were maintained in seawater from Coogee Beach in New South Wales. Experimental solutions were as above. Osmolarity was measured by cryoscopic osmometer (Osmomat 030, Gallay Scientific, North Melbourne, Victoria, Australia).

The cells were grown at a low light intensity of about 0.35 μmol sec^{-1} m^{-2}. At the time of the experiment, the cell illumination could be varied from light off (0.5 μmol sec^{-1} m^{-2}) to dim light (2.02 μmol sec^{-1} m^{-2}) or bright light (31.68 μmol sec^{-1} m^{-2}) provided by a fiber-optics light source. The light intensity was measured by quantum photometer (LI-COR LI-250, LI-COR, Lincoln, Nebraska, USA).

Cells were impaled and voltage-clamped by the two-electrode technique, and I/V curves obtained as described previously (Beilby & Bisson, 1999). Briefly, the cells were clamped to a bipolar staircase protocol generated by an LSI 11/73 computer with pulses of 100 msec separated by 250 msec at the resting membrane *PD* level. The last 10 points of each membrane *PD* and current staircase pulse were averaged to form the I/V profile (see Fig. 2*a*). The data-logging of each I/V profile took 8 sec. This experimental protocol is now referred to as "rapid I/V scan." Polynomials were fitted to the I/V data using Mathematica 3. Initially, each data set was fitted by a single polynomial, but if the fit was not satisfactory, the procedure was repeated for data segments varying from three points at a time to larger segments of up to ten points. Such fragmented fit had

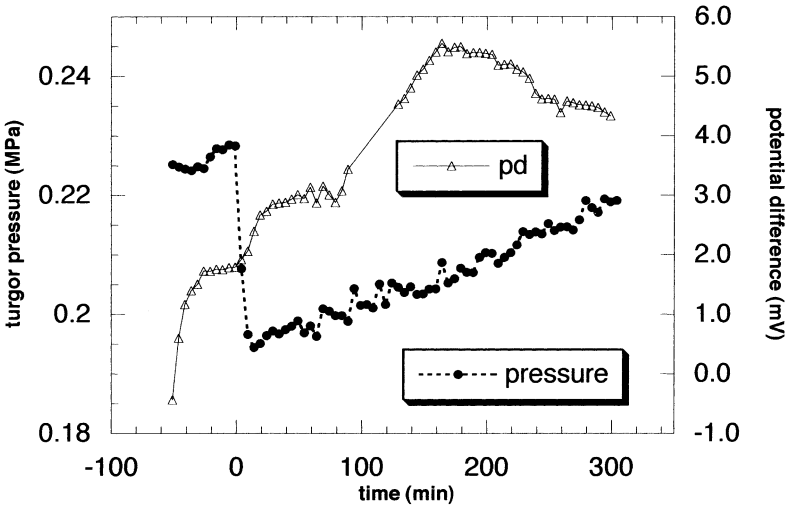

Fig. 1. Turgor pressure at the time of hypertonic stress and regulation (points connected by a dashed line). The hypertonic medium of +30 mOsmol·kg^{-1} was introduced at time 0. The vacuolar *PD* is shown as open triangles connected by a continuous line.

to be applied to the hypertonic data, as the I/V profiles exhibited sudden changes of slope. To aid in the analysis of two membranes in series, we generated R/V profiles, since two resistors in series are directly additive. The sum of the voltage drops across each membrane is equal to the clamp voltage, but the *PD* across each individual membrane is not known. $R(V)$ was obtained as the reciprocal of the $G(V)$ polynomial.

The vacuolar *PD* was also clamped for 12 sec (with 2 sec before and after each level at resting *PD*) to obtain the longer time dependence of the clamp currents. The resting *PD* was continuously monitored by a chart recorder in between the applications of both the rapid I/V and the long clamp protocols.

Results

Turgor Pressure in Resting State

Turgor pressure averaged 0.30 ± 0.026 MPa (mean ± SE, n = 18). There was no relation to cell size, with cell diameters ranging from 2.3 to 4.2 mm. However, cells that were doubly impaled tended to have a significantly lower turgor (p = 0.00806, Table 1). These cells were always impaled with the turgor probe first. Impalement by the second probe resulted in a drop in turgor, and these cells required a significantly (p = 0.027) longer time to come to steady state: 3–32 min for singly impaled, and 6–126 min for doubly impaled cells. We previously reported that cells that were doubly impaled for voltage clamping required 20 min or longer to come to steady state (*cf.* Figs. 3 and 4, Beilby & Bisson, 1999).

Hypertonic Regulation

Hypertonic stress of 30–100 mOsmol kg^{-1} was imposed on 11 cells, 3 of which were also impaled with a voltage-sensing electrode. Figure 1 shows an example of cell turgor pressure response to hypertonic medium of 30 mOsmol kg^{-1}. The cell turgor dropped within 7 min by 0.034 MPa. In this cell, the regulation started immediately and proceeded with an approximately linear trend of 9.7×10^{-5} MPa min^{-1}. The noise on the pressure trace resulted from adjusting the oil meniscus in the pressure probe (*see* Methods). The resting *PD* became more positive beginning immediately at a rate of 0.0194 mV min^{-1} to a maximum of 5.55 mV in 124 min, then declining to 4.34 mV at the end of the experiment. Cell responses to hypertonic challenge are summarized in Table 2. Out of 13 cells, 9 exhibited turgor regulation, ranging from 100% regulation in 215 min to 14% regulation to setpoint in 314 min. Some cells started regulation immediately (such as the cell in Fig. 1), others took up to 90 min to begin. Since many experiments were terminated before the turgor regulation was complete, due to blockage of the turgor probe or other difficulties, measuring the time to complete regulation was not feasible. For comparative purposes, we chose to measure the time to a given percent recovery. Since most cells recovered to at least 25% before termination of the experiment, we chose this as a comparison point. Cells required between 2.4 and 155 min to reach 25% recovery; the means were not significantly different between the singly and doubly impaled cells.

In the average of 3 cells, the resting *PD* became more positive in response to hypertonic stress by an average of 1.3 mV (*see* Table 2). Two cells with moderate *PD*s (1.79 mV and 2.78 mV) became more positive (to 5.5 mV and 5.80 mV, respectively), while 1 cell with a very positive *PD* (13.0 mV) became less positive (10.4 mV).

Figure 2*a* shows the *PD* and time dependence of the clamp currents at the time of hypertonic exposure to +100 mOsmol kg^{-1}, as the clamp command was changed from the resting *PD* (~9.0 mV) to levels of ±150 mV (——), ±100 mV (---) and ±50 mV (····). The series of long clamps was imposed on the cell between 17 and 30 min after initiation of the hyper-

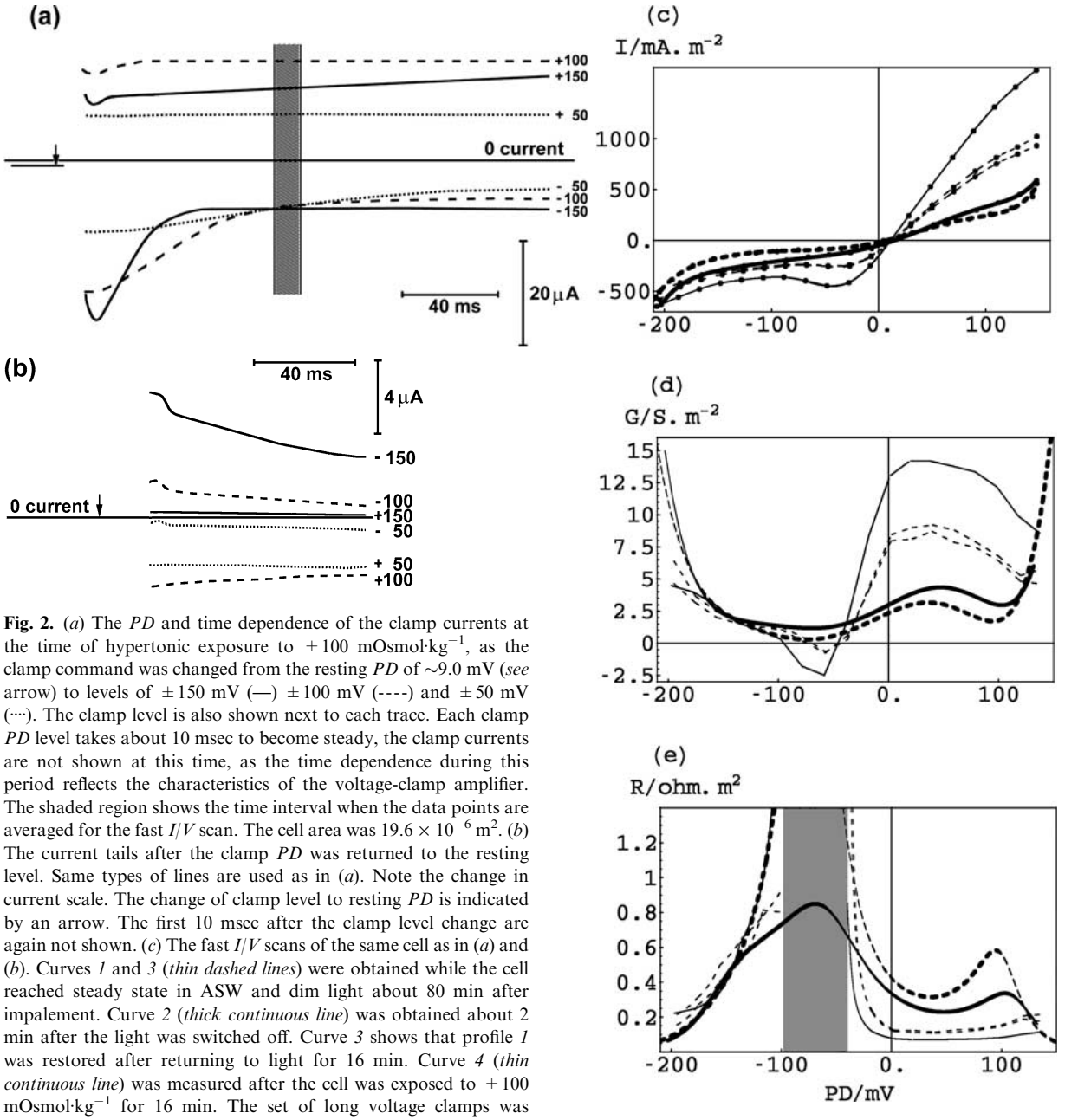

Fig. 2. (*a*) The *PD* and time dependence of the clamp currents at the time of hypertonic exposure to +100 mOsmol·kg^{-1}, as the clamp command was changed from the resting *PD* of ~9.0 mV (*see* arrow) to levels of ±150 mV (—) ±100 mV (----) and ±50 mV (····). The clamp level is also shown next to each trace. Each clamp *PD* level takes about 10 msec to become steady, the clamp currents are not shown at this time, as the time dependence during this period reflects the characteristics of the voltage-clamp amplifier. The shaded region shows the time interval when the data points are averaged for the fast *I*/*V* scan. The cell area was 19.6×10^{-6} m^2. (*b*) The current tails after the clamp *PD* was returned to the resting level. Same types of lines are used as in (*a*). Note the change in current scale. The change of clamp level to resting *PD* is indicated by an arrow. The first 10 msec after the clamp level change are again not shown. (*c*) The fast *I*/*V* scans of the same cell as in (*a*) and (*b*). Curves *1* and *3* (*thin dashed lines*) were obtained while the cell reached steady state in ASW and dim light about 80 min after impalement. Curve *2* (*thick continuous line*) was obtained about 2 min after the light was switched off. Curve *3* shows that profile *1* was restored after returning to light for 16 min. Curve *4* (*thin continuous line*) was measured after the cell was exposed to +100 mOsmol·kg^{-1} for 16 min. The set of long voltage clamps was performed after *I*/*V* curve *4* was obtained, and profile *5* (*thick broken line*) was obtained 8 min after the clamp to +150 mV. The *G*/*V* and *R*/*V* profiles calculated from the *I*/*V* profile are shown in (*d*) and (*e*), respectively. The shaded region shows undefined and negative resistance.

tonic exposure. The order of the voltage clamps was: −150, −100, −50, +50, +100 and +150 mV. At the time of each clamp, it took 10 msec for the *PD* to stabilize at each level and the currents are not shown for that period. The shaded bar depicts the time when the data points are averaged for the rapid *I*/*V* scans (as in part *c*). As the *PD* was clamped at more negative levels, the rate of current turnoff became faster. However, the *I*/*V* profile obtained by a fast *I*/*V* scan following within minutes of the long clamps showed no change to those run before the long negative *PD* clamps. In four cells tested, the clamp to positive *PD*s (100 to 150 mV) resulted in resting *PD* subsequently moving towards zero *PD* or becoming negative. The typical hypertonic *I*/*V* profile (obtained by fast scan) changed into more linear, less conductive characteristics. It took more than 30 min for the hypertonic profile to start to reappear. Clamps to negative *PD* levels during this time resulted in featureless time-independent currents (Fig. 3).

Figure 2*b* shows the current tails as the *PD* is returned to the resting level. Same types of lines are employed as in Fig. 2*a*. The first 10–15 msec after the *PD* level change are again lost due to clamp settling

Table 1. Turgor pressure and turgor regulation in singly and doubly impaled *Ventricaria* cells

	Steady-state turgor (MPa)	Time to steady state (min)	*n*
Singly-impaled cells	0.38 ± 0.027	13.8 ± 3.63	10
Doubly-impaled cells	0.19 ± 0.019	35.5 ± 13.7	8
All cells	0.30 ± 0.26	31.3 ± 9.4	18
	Change in turgor on 2nd impalement (MPa)	Potential difference (mV)	
Doubly-impaled cells	0.077 ± 0.024	1.4 ± 2.2	8

Singly impaled cells had only the pressure probe, doubly impaled cells had a pressure probe and a voltage-sensing electrode. Mean ± SE.

Table 2. Hypertonic response

	Change in π^o (MPa)	Change in turgor (MPa)	Percent regulation[a] (%)	Time to 25% reg.[b] (min)	Rate of reg.[c] (kPa/min)
Singly-impaled	0.202 ± 0.022 (9)	−0.186 ± 0.029 (9)	34 ± 8.0 (9)	99 ± 41 (6)	10.5 ± 5.48 (7)
Doubly-impaled	0.170 ± 0.038 (4)	−0.123 ± 0.031 (4)	33 ± 19 (4)	119 ± 36 (2)	0.27 ± 0.19 (2)
All cells	0.195 ± 0.0186 (13)	−0.165 ± 0.023 (13)	34 ± 7.8 (12)	104 ± 31 (8)	8.24 ± 5.22 (9)
	Change in *PD* (mV)	Time to change of *PD* (min)			
Doubly-impaled	1.3 ± 2.0 (3)	62 ± 61 (3)			

Total numbers are not the same as numbers in Table 1 because not all successfully impaled cells completed osmotic stress response. Mean ± SE (*n*).

[a] % of turgor lost that was regained by the end of the experiment. That is, % regulation (reg.) = $[1 - (|\text{turgor}^{\text{initial}} - \text{turgor}^{\text{final}}|/\text{turgor}^{\text{initial}})] \times 100$. Only one singly-impaled cell had come to an apparent steady turgor, with 79% regulation at 215 min. All other experiments were terminated before a new steady state was achieved, usually due to blockage or other failure of the probes.

[b] Time to regain 25% of turgor lost. Not all cells regained this much turgor during the period of measurement.

[c] Rate of regulation is the initial rate of regulation. In two cells the trace was not sufficiently clear to determine initial rate.

time. The tail currents were positive following the −150 mV clamp level, decreased greatly for −100 mV level and became negative for the −50 mV level, suggesting a reversal *PD* between −100 and −50 mV. We attempted to pinpoint the value of the reversal *PD* more accurately in other experiments, but it turned out to be difficult, as the tail currents became small and flat between about −60 mV and zero *PD*. This problem was compounded by a small offset current usually flowing as the cell *PD* was clamped at the resting level. The voltage clamp to +50 mV elicited a large and negative current tail, while the clamp to +100 mV produced only a slightly more negative current tail. Note the unexpected behavior of the current after the +150 mV pulse: small tail current in the opposite direction to that after clamp to +100 mV. Very similar trends were observed for current tails after all clamp levels in 3 other cells.

Figure 2*c* shows the fast scan *I*/*V* profiles from the same cell as in (*a*) and (*b*). Profile 1 (thin dashed line showing greater conductance) was obtained from the cell stabilized after an impalement in ASW in dim light. The data were fitted three points at a time to obtain the best fit. The profile 2 (thick continuous line) was an immediate response to light off (~2 min). The slope of this *I*/*V* profile was changing gradually, so only a single polynomial fit was necessary. The *I*/*V* characteristics were still flat 3 min after the dim light was switched back on (*not shown*). However, the *I*/*V* characteristics returned to dim-light steady-state 15 min later (profile 3, thin dashed line with lower conductance than profile 1, three points fitted at a time). The cell was then challenged by hypertonic medium (+100 mOsmol kg^{-1}), and developed a marked hypertonic profile after 15 min (curve 4, thin continuous line, three points fitted at a time). The sequence of long clamps (shown in part *a*) was then performed over a period of 18 min, with the +150 mV clamp last, resulting in subsequent damped oscillation of the free-running *PD* from a minimum of −5 mV to a maximum of +8 mV, settling on +5 mV after 8 min. The profile 5 (thick dashed line, single polynomial fit) was then recorded. Figure 2*d* and *e* show the *G*/*V* and *R*/*V* profiles, respectively, calculated from the *I*/*V* profiles.

Figure 3 shows the results of the long voltage clamps before (—) and after (----), for −100, −150 mV; (····), for +50, +100 mV) the hypertonic state was inactivated by prolonged voltage clamp to +150 mV. Note that the current tails for the negative clamps are similar before and after the clamp to +150 mV, but the current tails after the positive clamp levels are much smaller. The fast *I*/*V* scans (*not shown*) were similar to curves 1, 3 and 4 (Fig. 2*c*) before inactivation and to curves 2 and 5 (Fig. 2*c*) after inactivation.

Figure 4*a* follows the resting *PD* for 130 min after hypertonic exposure to +100 mOsmol kg^{-1}.

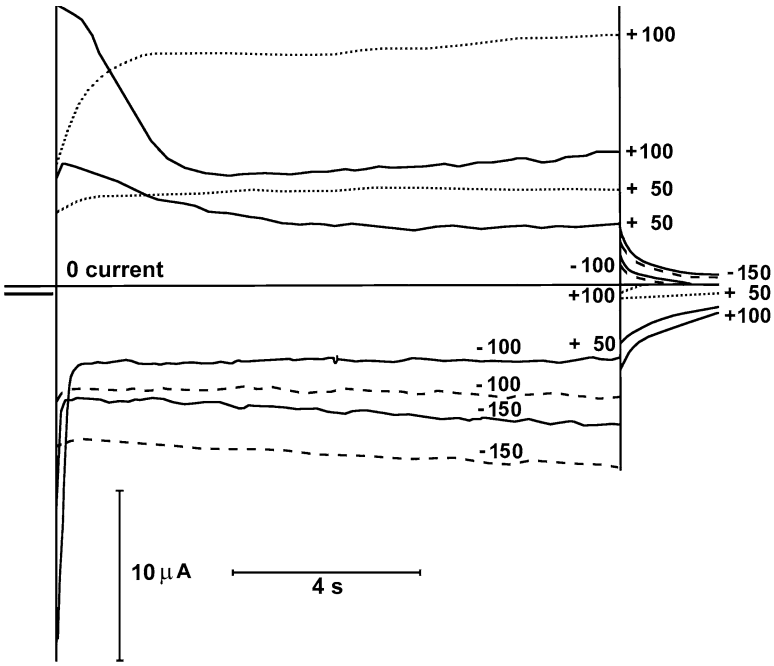

Fig. 3. Prolonged voltage clamps in cell undergoing hypertonic response, to +50, +100, −100 and −150 mV before (—) and after (----), −150, −100 mV; (····) +50, +100 mV) prolonged clamps to +150 mV, which inactivated the hypertonic state. Note the behavior of the current tails in each case.

The *PD* remained steady at 9 mV for 6 min, then became more positive, reaching a maximum of +14 mV after 30 min of the hypertonic medium. The *PD* then drifted to less positive 11 mV at the time of the last *I*/*V* scan of the experiment. The resting *PD* became transiently more positive as did the turgor probe-impaled cell in Fig. 1, although the time course was different. The numbered points in Fig. 4*a* signify the time of each *I*/*V* scan. Figure 4*b* shows fast *I*/*V* scans at these points throughout the regulation. Profiles *1* and *2* were fitted with single polynomials, profiles *2* to *5* were fitted by two polynomials (−150 to −50 mV and −50 to 100 mV) for the best fit. With time, the increase in conductance at ∼+50 mV (Fig. 4*c*) and increase in resistance at ∼−70 mV (Fig. 4*d*) developed, as is typical of the hypertonic state. Note that the most nonlinear *I*/*V* profile, with maximum conductance of 6 S m^{-2} (no. 3 in Fig. 4*c*) was observed after the resting *PD* started to decline. The summary of the electrical responses to hypertonic stress for the four cells tested in Sydney experiments is shown in Table 3. A relatively small number of cells was tested under hypertonic conditions, as their *I*/*V* characteristics were consistent with previous findings (Beilby & Bisson, 1999).

Hypotonic Regulation

Figure 5 shows the cell turgor response to making the medium hypotonic by −30 mOsmol kg^{-1}. The cell turgor increased within 2 min by 0.098 MPa, then started to decrease at an approximately linear rate of 3.2×10^{-4} MPa/min for the first 90 min. After this time the rate of regulation decreased. The vacuolar *PD* swung negative at the same time as the pressure increased. The most negative value of −7.8 mV was reached at 32 min. The *PD* underwent some small oscillations, while returning to more positive levels. Two out of a total of three cells exhibited hypotonic turgor regulation. Both cells started regulating within minutes after hypotonic stress, with a time to 25% regulation to setpoint of 69 ± 5 min (Table 4). One cell did not exhibit turgor regulation in 150 min.

Figure 6*a* shows the *PD* and time dependence of the clamp currents at 32 to 58 min of the hypotonic exposure to −100 mOsmol kg^{-1}. The clamp command was changed from the resting *PD* (−15 to −24 mV) to levels of ±150 mV (—) and −100 mV (----) and +100 mV (····). The currents in the hypotonic state showed a slow change and so all of the long clamp data sequence is shown. In contrast to the hypertonic state, the currents slowly increased under extreme voltages, both positive and negative. The current tails were smaller than in the hypertonic state and once again it was difficult to find a reversal *PD*. Figure 6*b* shows the effect of illumination on the fast *I*/*V* profiles after 20 min of hypotonic regulation in the same cell: profile *1* was measured in dim light, profile *2* (thick continuous line) was measured after two min of bright light and profile *3*, after two min back in dim light. Single polynomials were fitted to all the data. The resting *PD* became more negative by 15 mV and the conductance at the reversal *PD* nearly doubled (Fig. 6*b*). After the cell was returned to dim light, the resistance doubled (Fig. 3*c*). Note the difference of the before (*1*) and after (*3*) *I*/*V* profile. This

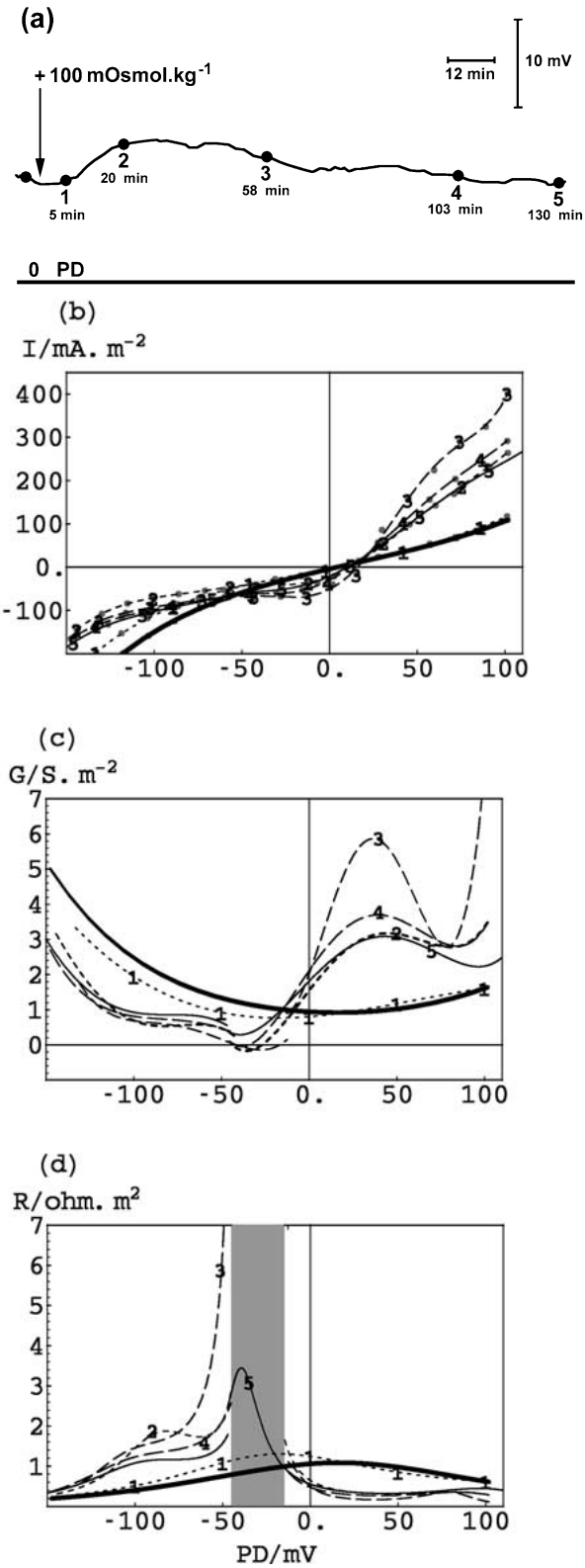

Fig. 4. (*a*) The resting *PD* after hypertonic exposure of +100 mOsmol·kg^{-1} (*see* arrow). The *PD* remained steady at 9 mV for 6 min, then became more positive, reaching the maximum of +14 mV after 30 min of the hypertonic medium. The numbered points signify the time of each fast *I*/*V* scan (after hypertonic exposure) shown in (*b*). The control *I*/*V* profile before the hypertonic stress (un-numbered point in part *a*) is shown as thick continuous line. The profiles after hypertonic shock are shown with progressively longer dashing. The *G*/*V* and *R*/*V* characteristics calculated from the *I*/*V* data are shown in (*c*) and (*d*), respectively.

behavior was observed in three different cells when the light intensity was changed at the time of hypotonic regulation.

Figure 7*a* follows the resting *PD* for 128 min after hypotonic exposure to −80 mOsmol kg^{-1}. The *PD* exhibited a small decrease at 6 min, but a large and rapid decrease started at 12 min. This rapid swing of the resting *PD* to negative values is similar to that exhibited by the turgor probe-impaled cell shown in Fig. 5, but there was a longer delay after the hypotonic exposure. The numbered points in Fig. 7*a* signify the times when the fast *I*/*V* scans were performed. Figure 7*b* shows the fast *I*/*V* scans throughout the regulation. Starting from a typical steady state *I*/*V* profile (thick continuous line, fitted three points at a time), the hypotonic *I*/*V* curves developed a high resistance between +50 and +150 mV (Fig. 7*d*) and high conductance (Fig. 7*c*) at negative *PD*s. The most negative reversal *PD* (profile 1, Fig. 7*b*) coincides with the highest conductance (Fig. 7*c*). The conductance then declined (except for profiles *3* and *4* near −150 mV), as the resting *PD* moved back towards its pre-regulation resting value. Profiles *1* to *6* were fitted with single polynomials. Table 3 shows that in the seven cells exposed to hypotonic challenge, the most negative-going reversal *PD* coincided with the highest conductance.

Similarly to the Buffalo experiments, in the Sydney experiments, the resting *PD* exhibited oscillations. Seven cells were exposed to hypotonic media with the osmolarity drop varying from 20 to 200 mOsmol kg^{-1} (*see* Table 3). The maximum *PD* excursion to negative levels generally became greater and the conductance increase more pronounced as the osmolarity drop increased. The limiting *PD* was −70 mV (at −200 mOsmol kg^{-1}), with conductance of 31 S.m^{-2} and very large currents, which saturated the amplifiers at 50 mV away from the reversal *PD*.

Discussion

Steady-State Turgor

Using the turgor probe, we measure a steady state turgor of 0.38 MPa for singly impaled cells, and 0.19 MPa for doubly impaled cells. Other measures in *Valonia* (*Ventricaria*) with the pressure probe gave values of 0.14 (Zimmermann & Steudle, 1970), 0.16 (Steudle & Zimmermann, 1971) and 0.1–0.2 MPa (Steudle & Zimmermann, 1980). Values calculated

Table 3. Electrical parameters from Sydney electrophysiological experiments

Cell no.	Osmotic stress ($mOsmol.kg^{-1}$)	Resting *PD* (mV)	Resting *G* ($S.m^{-2}$)	Delay before *PD* change (min)	*PD* (extreme) (mV)	Max *G* ($S.m^{-2}$)
Hypotonic						
937	−60	16.0	1.0	1.0	+5.0	0.5
	−200 (total)	16.0	1.0	immediate	−73.0	31.0
938	−200	7.0	4.0	17.0	−33.0	21.0
939	−80	14.0	6.5	6.0	−16.0	8.0
940	−100	9.0	17.0	6.0	−22.0	30.0
949	−200	15.0	1.0	5.0	−50.0	14.0
958	−100	3.0	10.0	5.0	−10.0	7.0
959	−100	16.0	8.0	9.0	−45.0	9.0
Mean ± SEM	−130 ± 21	12.0 ± 1.8	6.1 ± 2.0	6.25 ± 1.8	−30.5 ± 8.8	15.1 ± 4.0
Hypertonic						
954	+100	12.0	1.0	60	19.0	14.0
955	+100	17.0	7.0	no definite change	14.0	7.0
956	+100	4.0	3.0	6.0	10.0	18.0
957	+100	13.0	11.0	no definite change	14.0	11.0
Mean ± SEM	+100	11.5 ± 2.7	5.5 ± 2.2	16.5 ± 14.6	14.25 ± 1.8	12.5 ± 2.3

The osmotic change is produced by a change in NaCl concentration. The resting *PD* and resting conductance were measured minutes before the hypotonic or hypertonic exposure. The *PD* extreme is the most negative *PD* (hypotonic stress) or the most positive *PD* (hypertonic stress) at the time of regulation. Maximum *G* is obtained from the G/V profile at resting *PD* (as the *G* measurement is not continuous, this might not be the maximum conductance of the regulation process). The maximum *G* does not necessarily coincide with the *PD* extreme.

from the difference between internal and external osmotic pressure are similar (0.13; Hastings & Gutknecht, 1976). This is in the range of our doubly-impaled cells. These values for turgor are low compared to other species of algae, whether measured by the difference in osmotic pressure or with the turgor probe: the marine alga *Codium decorticatum* has a turgor pressure of 0.23 MPa and *Chaetomorpha* has a turgor of 1.5 MPa (Gutknecht, Hastings & Bisson, 1978). The freshwater Charophyte algae have a turgor pressure of about 0.5–0.8 MPa (Hope & Walker, 1975, Gutknecht et al., 1978). Higher plants have turgor in the range of 0.2–0.5 MPa (Steudle & Zimmermann, 1980), more similar to what we measured in the singly-impaled cells. While the lower turgor in the doubly-impaled cells requires more investigation (and may yield some insights into wounding response in *Ventricaria*), the steadying of the turgor after the second impalement (*see* Figs. 1 and 5), as well as the large response to the osmotic change, suggested that the cells were not badly damaged.

Models for Membrane Potential

Valonia (*Ventricaria*) cells are unusual in having a membrane potential that is positive, rather than negative. To date two models have been proposed to explain this. One is that the plasma membrane has a typically negative membrane potential, close to E_K and therefore probably dominated by potassium diffusion. The vacuole, however, is very positive with respect to the cytoplasm, caused by an electrogenic K^+ pump. This model was proposed by Damon (1930) and confirmed by Gutknecht (1966) and Davis (1981) who measured the membrane potential across the plasma membrane as negative and close to E_K. An alternative model was presented by Wang, Benz and Zimmermann (1995), who proposed that, as in *Acetabularia*, the plasma membrane *PD* might be generated by an electrogenic Cl^- transport system. However, their evidence is indirect, and our data, where comparatively small changes in the medium K^+ concentration cause large changes in the *I*/*V* profiles, (Beilby & Bisson, 1999) are consistent with the Damon/Gutknecht/Davis hypothesis. Note also that *Acetabularia* exhibits negative resting *PD* (near −200 mV), with hyperpolarization increasing as the pump is activated (Gradmann & Klemke, 1974), a very different behavior to that observed in *Ventricaria*.

Since the tonoplast is thought to contain unusual ion transporters, determining the electrophysiology of the separate membranes is very important for understanding of this system. We attempted to place the electrode in the cytoplasm. We obtained negative *PD*s in some experiments, but were unable to apply the voltage clamp. The resistances were too small and the cells were killed by the flow of large currents. We investigated the structure of *Ventricaria* cells with 6-carboxyfluorescein throughout the developmental stages from aplanospores to mature plants (Shepherd, Beilby, Cherry-Gaedt and Bisson, in preparation). The completion of the structural investigation is likely to result in a new model for *Ventricaria* transport. Since it is relevant to the electrophysiological analysis, we briefly summarize these results here. Optical sectioning using confocal laser scanning microscopy showed that the mature *Ventricaria* cells consist of

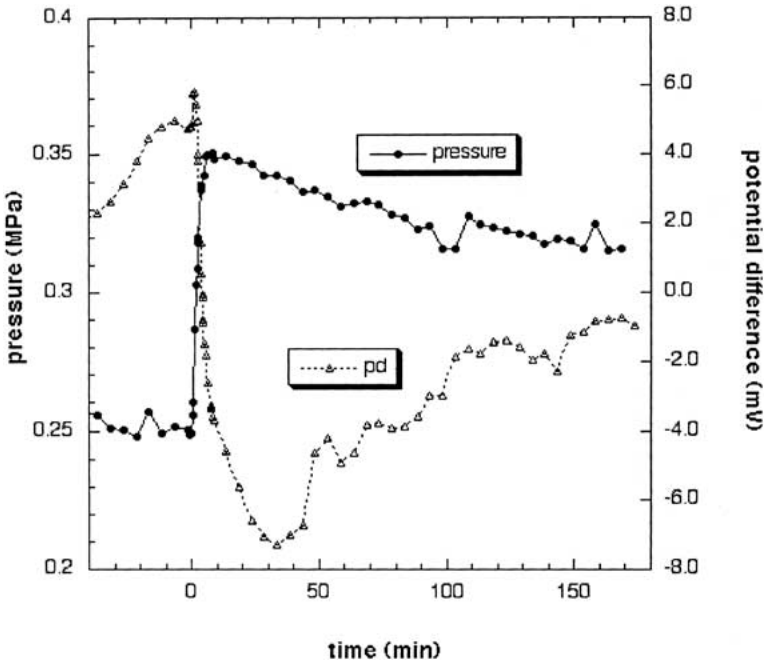

Fig. 5. Turgor pressure at the time of hypotonic stress and regulation (points connected by a continuous line). The hypotonic medium of −30 mOsmol.kg^{-1} was introduced at time 0. The vacuolar *PD* is shown as open triangles connected by a dashed line.

Table 4. Response of cells to hypotonic stress

Change in π^o (MPa)	Change in turgor (MPa)	Percent regulation (%)	Time to 25% reg. (min)	Rate of turgor regulation (kPa/min)	Change in *PD* (mV)	Time to change of *PD* (min)
−0.164 ± 0.030 (3)	0.54 ± 0.022 (3)	28 ± 15 (3)	69 ± 20 (2)	−0.33 ± 0.011 (2)	−7.3 ± 4.8 (2)	28 ± 5 (2)

All cells were doubly impaled.

aggregates of individual protoplasts, each containing a prominent nucleus, interconnected by thin cytoplasmic "bridges." These interconnections form the spongy structure of the cytoplasm, and are embedded in a complex vacuole, which frequently intervenes between cell wall and cytoplasm, and contains sulphated polysaccharides. The cytoplasm does not stream and appears quite solid. Upon strong hypertonic shock or mechanical vibration, the interconnections between the protoplast rupture and these might be observed as separate cells inside the mother cell. Consequently, the new model of *Ventricaria* might picture it as a tissue rather than a single cell. This very unusual structure makes the location of electrodes in the cytoplasm almost impossible. The preparation of cytoplasm-enriched fragments by centrifugation is also not feasible, as the cytoplasm is not fluid as in charophytes (Beilby & Shepherd, 1989). We will discuss the consequences of these anatomical discoveries on the analysis of the electrophysiological results in more detail in subsequent publications.

Turgor Regulation and Electrical Profiles

Beilby and Bisson (1999) identified the "pump on" *I*/*V* profile (see Fig. 2*c* or 7*b*) as steady state for cells acclimated to the experimental chamber for many hours in some experiments (much longer than it took for the turgor to reach steady value after impalement). Many plant cells, including most higher plants and freshwater algae, are characterized by an electrogenic H^+ ATPase at the plasma membrane that creates the electrochemical gradient for import of necessary nutrients (Smith & Raven, 1979; Spanswick, 1980; Hedrich & Schroeder, 1989). The H^+ pump-dominated *I*/*V* curves in *Chara* (Beilby & Walker, 1996) or guard cells (Blatt, 1987) exhibit negative *PD*s (near −200 mV) and a sigmoid profile resulting in a broad conductance peak near resting *PD*. The pump conductance on both sides of the maximum approaches zero, as the current through the pump becomes independent of change in *PD* (as modeled by Hansen et al., 1981). The *Ventricaria I*/*V* profile attributed to the pump state is very different, exhibiting a steep conductance decrease as the membrane is clamped to *PD*s between 0 and −100 mV (*see* Fig. 2*c* and *d*). The negative conductance region arises from strong *PD* dependence of the transporter current, which diminishes rather than coming to a constant value. The maximal conductance is near zero and decreases less sharply in the positive direction (+100 mV).

Marine algae show varied strategies to control membrane potential and transport ions (Raven,

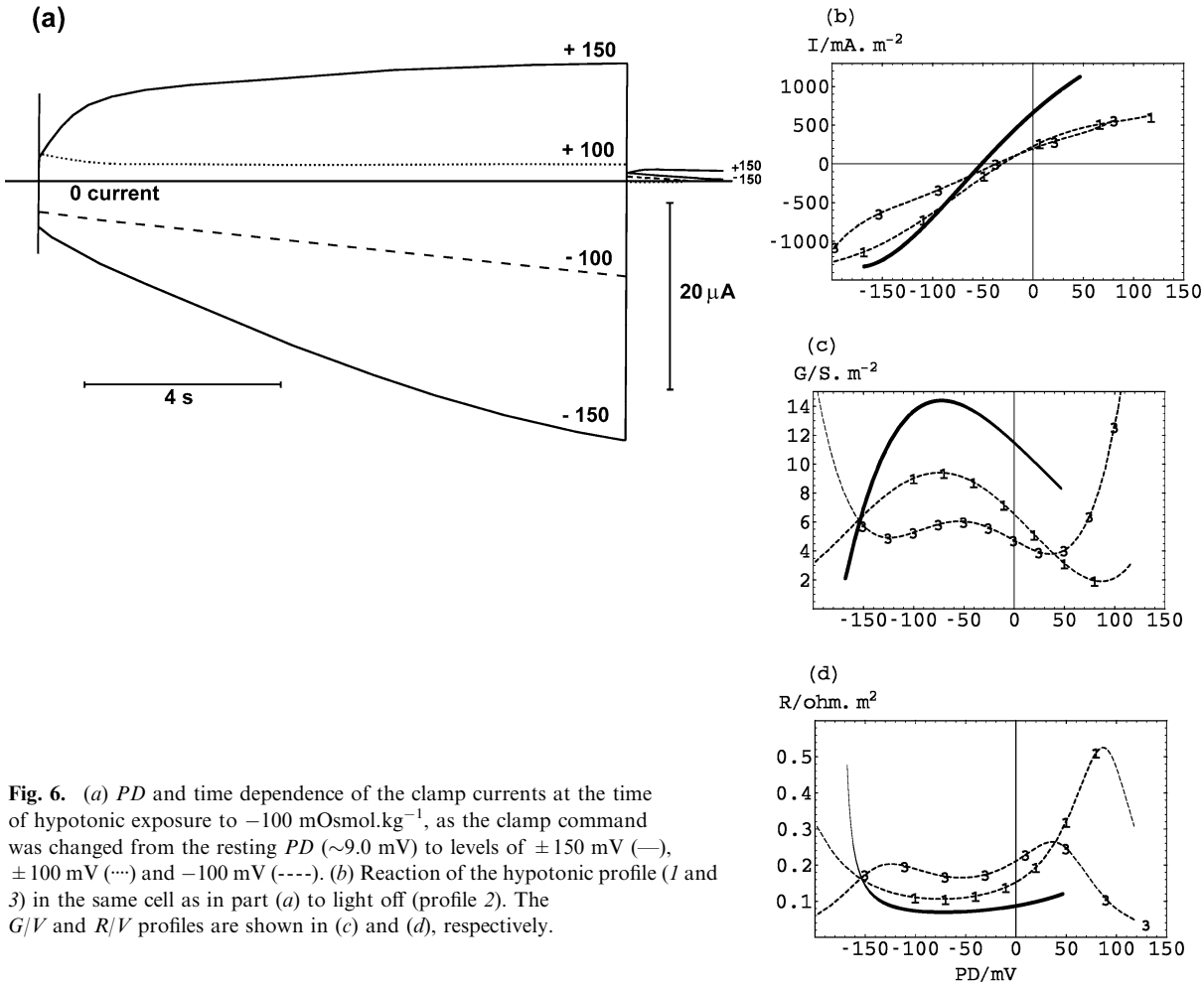

Fig. 6. (*a*) *PD* and time dependence of the clamp currents at the time of hypotonic exposure to −100 mOsmol.kg^{-1}, as the clamp command was changed from the resting *PD* (~9.0 mV) to levels of ±150 mV (—), ±100 mV (····) and −100 mV (----). (*b*) Reaction of the hypotonic profile (*1* and *3*) in the same cell as in part (*a*) to light off (profile *2*). The *G*/*V* and *R*/*V* profiles are shown in (*c*) and (*d*), respectively.

1975). Some, like *Codium*, show a K^+ diffusion potential similar to animal cells. Some, like *Valonia* and to a lesser extent *Griffithsia* and *Chaetomorpha*, have a more positive potential, apparently due to a more positive vacuolar *PD*. A few, like *Acetabularia*, have a more negative membrane potential, due to an inward electrogenic Cl^- pump with a sigmoid *I*/*V* profile, which can also be modeled by the Hansen et al. (1981) model.

Why don't marine algae have electrogenic H^+ pumps? It may be related to the fact that the ocean has a high pH and is well buffered by HCO_3^-, unlike freshwater and soil habitats, which are often significantly acidified. What is the purpose of the K^+ pump at the *Ventricaria* tonoplast (inner membrane) while the cell is in the steady state? It must be compensating for passive efflux of K^+ out of the vacuole, which does not have a strong impact on the electrical characteristics.

Hypertonic Regulation

The turgor pressure in 9 out of 11 cells was found to increase toward the setpoint after hypertonic shock. In 2 out of the 3 cells, in which *PD* was measured simultaneously with turgor pressure, vacuolar *PD* became more positive at some time during regulation (Table 2). In cells that were impaled with a voltage-sensing and a current-injecting electrode (Table 3), 3 out of 4 cells became more positive. In each case, the cells with the most positive *PD* initially did not become more positive.

These results are consistent with our previous proposal (Beilby & Bisson, 1999) that the increasing non-linearity in the fast scan *I*/*V* profile reflects the activation of the importer of K^+, the putative K^+ pump. The "pump on" state *I*/*V* typical of hypertonic response contains two main features: a resistance peak near −100 mV (Fig. 2*e*) and a conductance peak near +50 mV (Fig. 2*d*). We propose that the greater the conductance peak, the higher the rate of pumping. The negative conductance region (resulting in undefined resistance) reflects the rate of pump inactivation as the *PD* goes negative (see Fig. 2*a*).

The hypertonic *I*/*V* state is characterized by high conductance at positive *PD*s (Fig. 4*c*) and high resistance at negative *PD*s (Fig. 4*d*). However, closer examination of the results reveals that the increase in conductance is not simply related to the vacuolar *PD*

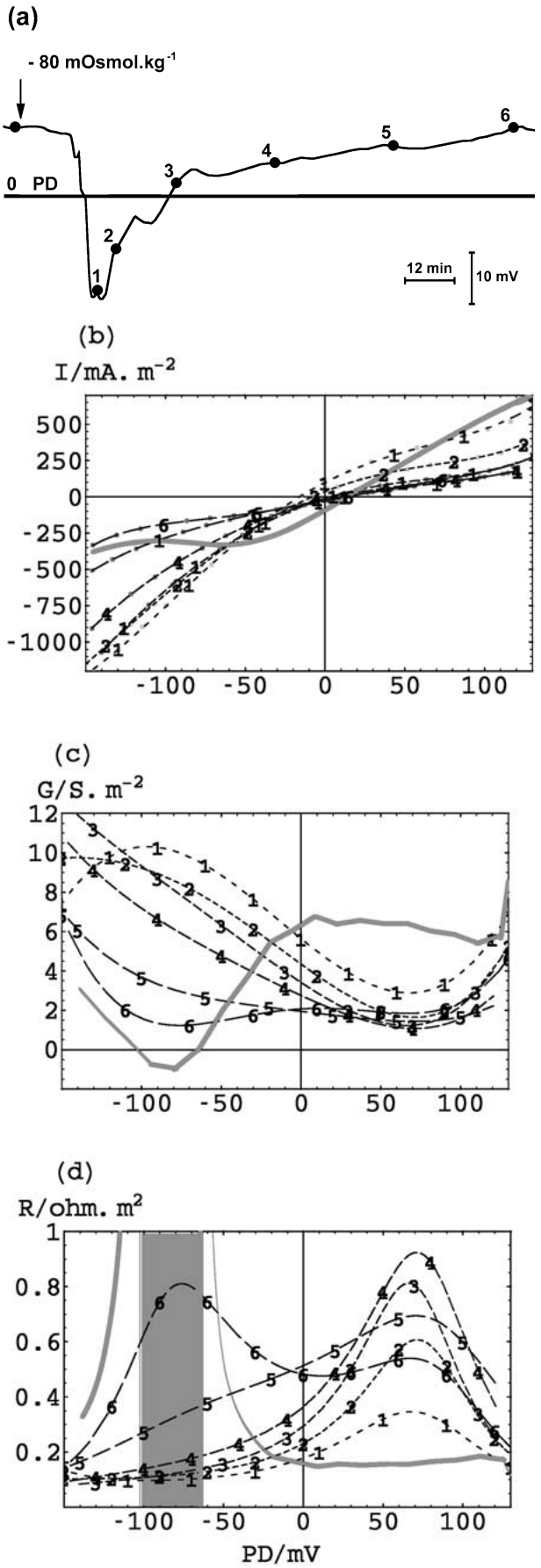

nor to the process outcome, turgor return to the setpoint. In Fig. 1, turgor regulation proceeds linearly with time, not reflecting the changes in vacuolar *PD*. In all three cells in which turgor and *PD* were measured simultaneously, the highest degree of turgor regulation was not correlated with maximum positive *PD*. One cell, for instance, required 88 min to achieve 25% regulation toward setpoint, while another required only 44. However, the first cell became 12 mV more negative, while the second cell became only 4 mV more negative. The turgor increase involves integration over the cell surface and inflow of all the osmotica: Cl^- and Na^+ as well as K^+. These integrative processes may even out the fluctuations. On the other hand, Fig. 2*c* and Table 3 show that the vacuolar resting *PD* can stay almost unchanged, while the resting conductance can quadruple (Fig. 2*d*). In the course of the hypertonic response, shown in Fig. 4, the most conductive fast I/V profile was observed after the resting *PD* had gone through the maximum. So the resting *PD* going more positive does not necessarily imply greater conductance and, presumably, a harder working pump. In this respect the *Ventricaria* pump behaves differently from the H^+ pump of the charophytes and higher plants and from the Cl^- pump of *Acetabularia*, where the greater pump conductance means more hyperpolarized (negative) resting *PD*.

The cells showed great variability in the onset and rate of turgor regulation. The presence of the thick mucilage, containing sulphated polysaccharides, modulates the speed and manner of turgor regulation in salt-tolerant charophyte *Lamprothamnium* (Shepherd, Beilby & Heslop, 1999; Shepherd & Beilby, 1999). In future experiments the mucilage thickness will be recorded for *Ventricaria* cells. The presence of the mucilage also explains the rather slow response to both hyper- and hypotonic shocks (Figs. 1 and 5).

Hypotonic Regulation

The relationship between the turgor regulation and vacuolar *PD* (Fig. 5) is again not direct, since turgor regulation continues at a constant rate, while the *PD* peaks and begins to return to a less negative potential. However, there is a good correspondence between the vacuolar *PD* and conductance: the more negative the *PD*, the greater the conductance at the

Fig. 7. (*a*) The resting *PD* after hypotonic exposure to −80 mOsmol·kg^{-1} (*see* arrow). The numbered points signify the times when the fast I/V scans were performed. (*b*) The fast I/V scans throughout the regulation, depicted by lines of increasingly longer dashing. The G/V and R/V profiles are shown in (*c*) and (*d*), respectively. The steady-state I/V profile has hypertonic characteristics (*thick continuous line*).

reversal *PD* tends to be (Table 3). The maximum negative *PD* that we observed during hypotonic response was −70 mV (Table 3), similar to that estimated across the plasmalemma (outer membrane). We propose that hypotonic regulation is channel-mediated, as the K^+ channels on the tonoplast (inner membrane) are probably activated by negative *PD*.

The Time-Dependence of the Current

Does the shift in the *I*/*V* profile during hypertonic regulation reflect changes in the state of each pump or changes in the pump number? The long voltage clamps confirm in more detail what the fast *I*/*V* scans indicate: the K^+ pump current inactivates within tens of msec (Fig. 2*a*), as the *PD* becomes more negative than −50 mV. However, clamping the *PD* at negative levels inactivates the pump only temporarily and subsequent *I*/*V* scans performed minutes later once again show the "pump-on" state. Therefore, as the vacuolar *PD* becomes negative at the time of the hypotonic regulation (Fig. 5), the pump is inactivated, but it re-activates promptly if the *PD* rises above −50 mV. More unexpected is the longer-term inhibition by long clamps to positive *PD*s, which the cell membrane is unlikely to experience during its normal life on the reef. As outlined above, the K^+ pump *I*/*V* profile is rather different from that of the H^+ pump, where the current approaches a constant value at very negative or very positive *PD* values (*see*, for instance, Beilby & Walker, 1996).

The tail current analysis (such as shown in Fig. 2*b*) suggests that the positive tail currents probably flow through inward rectifying channels on both membranes, which are closed by positive membrane *PD*s. In Fig. 3 these tails after negative clamp levels are unchanged before and after the inhibitory positive clamp. The tails after the positive clamp levels are inhibited and may be associated with the K^+ pump current (Fig. 3).

The long voltage clamps under hypotonic stress show very different results. Here, the currents activate rather than inactivate over time, with more pronounced activation at more extreme potentials (*see* Fig. 6*a*). The data shown in this figure were collected after the hypotonic medium flowed through the chamber for more than 30 min. Therefore, the slow increase in the current is not likely to arise from mixing of ASW and hypotonic medium. Our structural studies revealed a sulfated polysaccharide mucilage on the *Ventricaria* cell surface, which could behave as an unstirred layer with selective ion exchange properties (Siegel et al., 1996). However, the slow current increase at −150 mV was seen in both hypotonic cells tested and in none of the four hypertonic cells investigated. The influence of the mucilage will be investigated in future experiments.

While these long *I*/*V* scans for both hypertonic and hypotonic responses reveal more information about the potential dependence of membrane transporters, some of these effects seem to be only slowly (or not at all) reversible (Fig. 2*c–e*), sometimes leading to cell death (Beilby & Shepherd, 2001). Consequently, once the long time behavior of the currents have been assessed, the rapid *I*/*V* scan is the best tool for effects such as turgor regulation, where the cells are monitored for up to 10 hr.

Light Effects

Figure 2*c–e* compares the "pump-off" profiles following the +150 mV prolonged clamp and decrease of illumination during hypertonic regulation. We see that decreasing illumination flattens the *I*/*V* curve, indicating that the pump is inhibited in the absence of light. This is consistent with other studies showing pump inhibition in the dark. Shabala and Newman (1999) found in bean leaves that an influx of Ca^{2+} is the first response to increased intensity of illumination, followed by increased H^+ efflux several min later. The authors suggest that the H^+ ATPase might be stimulated by an increase in calcium concentration in the cytoplasm. A similar stimulation of an electrogenic pump by calcium has been reported in *Neurospora* (Lew, 1989). Is the K^+ pump stimulated by such an increase in calcium concentration? This hypothesis will be investigated in future experiments.

The increase in conductance upon greater light intensity in hypotonic conditions (Fig. 6*b–d*) was somewhat unexpected. We hoped to distinguish the pump-generated conductance from the channel conductance by the dependence on illumination intensity. However, data in Fig. 6*b–d* suggest either that the channels are light sensitive or that the pump does run in reverse, contributing to the turgor regulation (Zimmermann & Steudle, 1974). There are light-sensitive channels in zygotes of the brown algae *Fucus* and *Pelvetia*, (Love, Brownlee & Trewavas, 1997) as well as in land plants such as *Arabidopsis* (Spalding, 2000), so this possibility cannot be neglected.

Signaling

How the signal for either hypertonic or hypotonic stress is transmitted from the plasmalemma (outer membrane), where it must be detected, to the tonoplast (inner membrane), where transporters responsible for turgor regulation reside, remains to be elucidated. The electrical response to a change in turgor is more rapid than the response to alterations in external K^+ concentrations (Beilby & Bisson, 1999). This suggests that the response to altered K^+ concentrations is moderated by slow changes in the

cytoplasm, such as changes in cytoplasmic K^+ concentration, while a much more rapid signaling system responds to changes in turgor. The nature of this signaling system will be addressed in future investigations.

This research was supported in part by NSF grant INT9605130 to MAB and by two grants by ARC (Australian Research Council) to MJB. We thank S. Santos for his help in culturing the *Ventricaria*. We also thank Prof. AWD Larkum, Acting Director of Sydney University Biological Informatics and Technology Center, and Mr. R. Forbes, Laboratory Manager of Heron Island Research Station, for supplying the *Ventricaria* cells. We are grateful to Great Barrier Reef Marine Park Authority for granting the permit for *Ventricaria* collection.

References

Beilby, M.J. 1984. Current-voltage characteristics of the proton pump at *Chara* plasmalemma: I. pH dependence. *J. Membrane Biol.* **81:**113–125

Beilby, M.J. 1986. Factors controlling the K^+ conductance in *Chara*. *J. Membrane Biol.* **93:**187–193

Beilby, M.J., Bisson, M.A. 1999. Transport systems of *Ventricaria ventricosa*: *I/V* analysis of both membranes in series as a function of $[K^+]_o$. *J. Membrane Biol.* **171:**63–73

Beilby, M.J., Shepherd, V.A. 1989. Cytoplasm-enriched fragments of *Chara*: structure and electrophysiology. *Protoplasma* **148:**150–163

Beilby, M.J., Shepherd, V.A. 2001. Modeling the current-voltage characteristics of charophyte membranes. II. The effect of salinity on membranes of *Lamprothamnium papulosum*. *J. Membrane Biol.* **181:**77–89

Beilby, M.J., Walker, N.A. 1996. Modelling the current-voltage characteristics of *Chara* membranes: I. The effect of ATP removal and zero turgor. *J. Membrane Biol.* **149:**89–101

Blatt, M.R. 1987. Electrical characteristics of stomatal guard cells: the contribution of ATP-dependent, "electrogenic" transport revealed by current-voltage and difference-current-voltage analysis. *J. Membrane Biol.* **98:**257–274

Blom-Zanstra, M., Koot, H., van Hattum, J., Vogelzang, S.A. 1997. Transient light-induced changes in ion channel and proton pump activities in the plasma membrane of tobacco mesophyll protoplasts. *J. Exp. Bot.* **48:**1623–1630

Damon, E.B. 1930. Dissimilarity of inner and outer protoplasmic surfaces in *Valonia*. *J. Gen. Physiol.* **13:**207–221

Davis, R.F. 1981. Electrical properties of the plasmalemma and tonoplast in *Valonia ventricosa*. *Plant. Physiol.* **67:**825–831

Fujii, S., Shimmen, T., Tazawa, T. 1979. Effect of intracellular pH on the light-induced potential change and electrogenic activity in tonoplast-free cells of *Chara australis*. *Plant Cell Physiol.* **20:**1315–1328

Gradmann, D., Klemke, W. 1974. Current-voltage relationship of the electrogenic pump in *Acetabularia*. *In:* Membrane Transport in Plants. U. Zimmermann, J. Dainty, eds. pp. 131–138 Springer, New York

Guggino, S., Gutknecht, J. 1982. Turgor regulation in *Valonia macrophysa* following acute osmotic shock. *J. Membrane Biol.* **67:**155–164

Guillard, R.R.L., Ryther, J.H. 1962. Studies of marine planktonic diatoms. I. *Cyclotella nana* husted1 and *Detonula confervacea* (Cleve) gran. *Can. J. Microbiol.* **8:**229–239

Gutknecht, J. 1966. Sodium, potassium, and chloride transport and membrane potentials in *Valonia ventricosa*. *Biol. Bull.* **130:**331–344

Gutknecht, J., Hastings, D., Bisson, M. 1978. Ion transport and turgor pressure regulation in giant algal cells. *In:* Membrane Transport in Biology. Vol. III. Transport Across Multimembrane Systems. Giebisch, G., Tosteson, D.C., Ussing, G., eds., pp. 125–174. Springer, Berlin

Hansen, U.-P., Gradmann, D., Sanders, D., Slayman, C.L. 1981. Interpretation of current-voltage relationships for "active" ion transport systems: I. Steady-state reaction-kinetic analysis of class-I mechanisms. *J. Membrane Biol.* **63:**165–190

Hastings, D.F., Gutknecht, J. 1974. Turgor pressure regulation: Modulation of active potassium transport by hydrostatic pressure gradients. *In:* Membrane Transport in Plants. Zimmermann, U., Dainty, J., eds. pp. 79–83. Springer, New York

Hastings, D.F., Gutknecht, J. 1976. Ionic relations and the regulation of turgor pressure in the marine alga, *Valonia macrophysa*. *J. Membrane Biol.* **28:**263–275

Hedrich, R., Schroeder, J. 1989. The physiology of ion channels and electrogenic pumps in higher plants. *Annu. Rev. Plant Physiol. Plant Mol. Biol.* **40:**539–569

Hope, A.B., Walker, N.A. 1975. The Physiology of Giant Algal Cells. Cambridge University Press

Lew, R.R. 1989. Calcium activates an electrogenic proton pump in *Neurospora* plasma-membrane. *Plant Phsyiology* **91:**213–216

Love, J., Brownlee, C., Trewavas, A.J. 1997. Ca^{2+} and calmodulin dynamics during photopolarization in *Fucus serratus* zygotes. *Plant Physiology* **115:**249–261

Olsen, J.L., West, J.A. 1988. *Ventricaria* (Siphonocladales-Cladophorales complex, Chlorophyta), a new genus for *Valonia ventricosa*. *Phycologia* **27:**103–108

Raven, J.A. 1975. Algal Cells. *In:* Ion Transport in Plant Cells and Tissues. Baker, E., Hall, A., eds. pp. 125–160. North Holland, Amsterdam

Serrano, E.E., Zeiger, E., Hagivara, S. 1988. Red light stimulates an electrogenic proton pump in *Vicia* guard cell protoplasts. *Proc. Nat. Acad Sci. USA* **85:**435–440

Shabala, S., Newman, I. 1999. Light-induced changes in hydrogen, calcium, potassium, and chloride ion fluxes and concentrations from the mesophyll and epidermal tissues of bean leaves. Understanding the ion basis of light-induced bioelectrogenesis. *Plant Physiol.* **119:**1115–1124

Shepherd, V.A., Beilby, M.J. 1999. The effect of an extracellular mucilage on the response to osmotic shock in the charophyte alga *Lamprothamnium papulosum*. *J. Membrane Biol.* **170:**229–242

Shepherd, V.A., Beilby, M.J., Heslop, D.J. 1999. Ecophysiology of the hypotonic response in the salt-tolerant alga *Lamprothamnium papulosum*. *Plant Cell Environ* **22:**333–346

Siegel, G., Malmsten, M., Wenzel, K., Kauschmannm, A., Klubendorf, D. 1996. Physicochemical and medical implications of a blood flow sensor. In: Proceedings of the International Membrane Science and Technology Conference (ed. Fane, A.G.) UNESCO Center for Membrane Science and Technology, Sydney, Australia

Smith, F.A., Raven, J.A. 1979. Intracellular pH and its regulation. *Annu. Rev. Plant Physiol.* **30:**238–311

Spalding, E.P. 2000. Ion channels and the transduction of light signals. *Plant Cell Environ.* **23:**665–674

Spanswick, R.M. 1980. Biophysical control of electrogenic pumps in the *Characeae*. *In:* Plant Membrane Transport: Current Conceptual Issues. Spanswick, R.M., Lucas, W.J., Dainty, J., eds. pp. 305–313. Elsevier/North Holland Biomedical

Stento, N.A., Ryba, N., Gerber, Kiegle, E.A., Bisson, M.A. 2000. Turgor regulation in the salt-tolerant alga *Chara longifolia*. *Plant Cell Env.* **23:**639–637

Steudle, E., Zimmermann, U. 1971. Hydraulische Leitfähigkeitvon *Valonia utricularis*. *Z. f. Naturforschung* **26:**1302–1311

Steudle, E., Zimmermann, U. 1980. Fundamental water relations parameters. *In:* Plant Membrane Transport: Current Conceptual Issues. Spanswick, R.M., Lucas, W.J., Dainty, J., eds. pp. 113–127. Elsevier/North-Holland Biomedical Press

Wang, J., Benz, R., Zimmermann, U. 1995. Effects of light and inhibitors of ATP-synthesis on the chloride carrier of the alga *Valonia utricularis*: is the carrier a chloride pump? *Biochem. Biophys. Acta* **1233:**185–197

Zimmermann, U., Steudle, E. 1970. Bestimmung von Reflexionskoeffizienten an der Membran der Alge *Valonia utricularis*. *Z. f. Naturforschung* **25:**500–504

Zimmermann, U., Steudle, E. 1974. The pressure dependence of the hydraulic conductivity, the membrane resistance and membrane potential during turgor pressure regulation in *Valonia utricularis*. *J. Membrane Biol.* **16:**331–352